Electronic and Magnetic Properties of Quasifreestanding Graphene on Ni

A. Varykhalov,[1] J. Sánchez-Barriga,[1] A. M. Shikin,[2] C. Biswas,[1] E. Vescovo,[3] A. Rybkin,[2] D. Marchenko,[2] and O. Rader[1]

[1]*BESSY, Albert-Einstein-Str. 15, D-12489 Berlin, Germany*

[2]*V. A. Fock Institute of Physics, St. Petersburg State University, 198504, St. Petersburg, Russia*

[3]*National Synchrotron Light Source, Brookhaven National Laboratory, Upton, New York 11973-5000, USA*

(Received 15 March 2008; published 10 October 2008)

For the purpose of recovering the intriguing electronic properties of freestanding graphene at a solid surface, graphene self-organized on a Au monolayer on Ni(111) is prepared and characterized by scanning tunneling microscopy. Angle-resolved photoemission reveals a gapless linear π-band dispersion near $\bar{K}$ as a fingerprint of strictly monolayer graphene and a Dirac crossing energy equal to the Fermi energy (E_F) within 25 meV meaning charge neutrality. Spin resolution shows a Rashba effect on the π states with a large (~13 meV) spin-orbit splitting up to E_F which is independent of $\mathbf{k}$.

DOI: 10.1103/PhysRevLett.101.157601 PACS numbers: 73.20.At, 71.70.Ej, 79.60.Dp, 81.05.Uw

Since its successful isolation by exfoliation from graphite samples [1], graphene has been among the most promising materials for future electronic devices. In fact, there are separate developments in the realms of electronic transport and magnetoelectronics where this material excels: A remarkable conductivity with room-temperature mobilities of up to 1.5×10^4 cm^2/V s was observed and a half-integer quantum Hall effect indicates the presence of relativistic charge carriers with vanishing mass [2–4]. It has been shown that the behavior of these massless Dirac fermions satisfies the laws of quantum electrodynamics, and the high mobilities may provide the basis for an extremely fast graphene-based electronics [2,5]. Alkali adsorption experiments have demonstrated the effect an external electric field would exercise on electronic structure and band gap [6], and this prediction was confirmed by transport measurements of a graphene bilayer [7] thus presenting a key ingredient for an efficient graphene-based transistor.

An acceleration of electronic devices is further expected from spintronics, where signal transmission is not achieved via transport of charge but spin. Graphene is being assigned a role in spintronics since spin current manipulation was demonstrated in carbon nanotubes [8] and the realization of a spin valve was reported based on graphene [9]. The freestanding graphene sheet bridging permalloy and Au contacts leads to a 10% change in room-temperature resistance when the permalloy magnetization is reversed. This has been interpreted as successful spin injection into and efficient spin transport by the graphene [9]. With an extra oxide tunneling barrier between graphene and the ferromagnet, a large spin relaxation length of 1.5–2.0 μm was obtained [10].

Recent photoemission investigations of a graphene monolayer on SiC indicate that the quasiparticle picture used to describe electron correlation in graphite [11] remains valid for the Dirac fermions in graphene and that photoemission investigations are therefore particularly valuable for assessing the electronic properties and possible applications of graphene [12].

These investigations as well as the applications would benefit from a more practical and reliable method than mechanical exfoliation [1] to prepare continuous graphene sheets. One way to produce ultrathin graphite layers is the controlled evaporation of Si from heated SiC [13,14]. Transport properties have been investigated in 3-monolayer-thick (ML) graphite films grown in this way which furthermore allows for lithographical patterning and conductance modulation by a gate electrode [15]. The relativistic charge carriers observed for freestanding graphene were observed in graphitized SiC as well [15]. It is, however, difficult to control the thickness when graphitizing SiC by Si evaporation, and it is known that the half-integer quantum Hall effect disappears already for a freestanding film of two graphene layers [2]. Band structure measurements by photoemission were at first performed on films thicker than one monolayer [6,16], and truly monolayer graphene was achieved on SiC only most recently [12].

We pursue a very different way of producing a single graphene layer and decoupling it from its substrate. The method involves graphitization of Ni followed by intercalation of Au [17]. While it has been established experimentally [17] and theoretically [18] that electronic binding energies in graphene on bare Ni differ largely (~2 eV) from those in bulk graphite, successive Au intercalation, i.e., introduction of Au atoms into the interface between graphene and Ni, saturates the Ni3d bonds and weakens the chemical interaction between the graphene adlayer and its substrate as confirmed by phonon spectra [19]. This results in a shift of electronic π and σ states towards lower binding energies [17].

In the present Letter, we investigate the electronic structure of the graphene monolayer on Ni(111) intercalated with Au by angle-resolved photoemission in the vicinity of the Fermi energy (E_F). Its is demonstrated that this preparation which employs self-organization takes the system closer to ideal freestanding graphene than any other preparation on a solid substrate before, in particular, we will reveal seven key properties of our system: (i) The π band

shows a linear dispersion indicating relativistic quasiparticles. (ii) Its constant-energy surfaces are conical, noncircular, and asymmetric in photoemission intensity. (iii) It touches the Fermi edge precisely at the Dirac crossing point E_D. This behavior has not been seen in photoemission as yet. The only monolayer data of graphene/SiC available obtain E_D 0.45 eV below E_F [12]. (iv) The graphene is gapless. Residual interaction with the Au is revealed by (v) a kink in the $E(k)$ dispersion and (vi) a predominantly threefold symmetry in scanning tunneling microscopy (STM). We show that (vii) the π states near $\bar{K}$ are spin dependent with a large spin-orbit splitting causing a spin-polarized Fermi surface.

Experiments were performed with hemispherical electron energy analyzers and linearly polarized undulator radiation using different setups at BESSY: Scienta SES100 at U125/2-SGM, Scienta R4000 at UE112-PGM2b, SPECS Phoibos 150 at UE112-PGM1 and PGM2a. For spin analysis, a Rice University Mott-type spin polarimeter has been operated at 26 kV [20]. The spin quantization axis is in the surface plane of the sample and perpendicular to $\mathbf{k}_\parallel$, i.e., to the surface-projected electron wave vector. The Ni(111) surface has alternatively been prepared by cycles of Ar^+ sputtering and heating of a Ni single crystal and by deposition of 15 ML Ni from an e^--beam evaporator onto W(110) and annealing. The base pressure was 1–2 $\times$ 10^{-10} mbar. The W(110) crystal has been prepared by heating in oxygen and flashing to high temperature. The graphene layer was formed in a partial C_3H_6 pressure of 1×10^{-6} mbar with the sample held at 800 K during 5 min. A considerable advantage over other techniques of graphene preparation is that the graphitization of Ni is a self-terminating process which stops after a single layer of graphene has formed. Surface preparation, graphitization, and sample orientation have been monitored by low-energy electron diffraction *in situ* and by STM in a separate chamber. Figure 1(b) shows STM images of the resulting graphene layer. Unlike other Ni surfaces, Ni(111) generates graphene in registry with its own lattice [Fig. 1(a)], and the two different carbon adsorption sites A and B lead to threefold symmetry in the STM [Fig. 1(b)]. The structural model of Fig. 1(a) has recently been confirmed by theory [18]. Au was evaporated from a Au-covered W wire by Ohmic heating, and intercalation of 1 ML Au was achieved by short annealing at 600–700 K. Figure 1(c) reveals a superstructure and weaker $A - B$ contrast in a predominantly threefold symmetry.

Figure 2 displays angle-resolved photoemission data of the $E(\mathbf{k}_\parallel)$ band dispersion along the $\overline{\Gamma K}$ direction of the graphene Brillouin zone (a) before and (b) after intercalation of a full monolayer of Au. The bands have shifted nonrigidly towards E_F by $\sim$2 eV in average. No traces of unshifted bands are seen in Fig. 2(b) which means that the intercalation is complete—a remarkable finding in view of a macroscopic probing area of typically 0.1 mm^2 over which the photoemission measurement averages. This is due to the fact that intercalation of Au is self-limiting as well because it allows for intercalation of only one atomic layer of Au. The Au blocks the chemical interaction between graphene and Ni(111), and the charge state of the system changes towards the one of freestanding graphene.

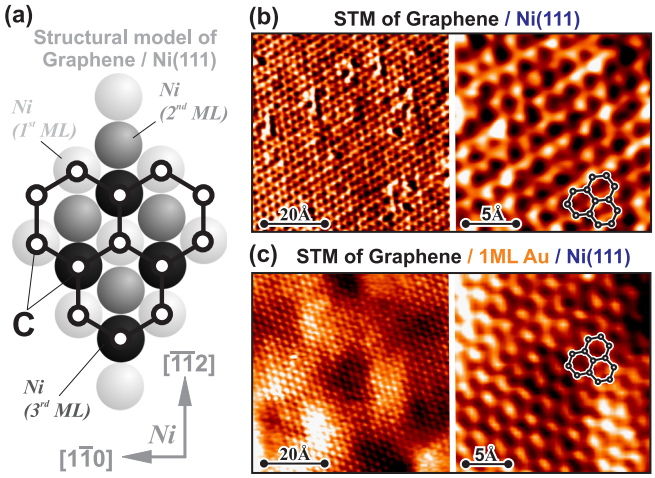

FIG. 1 (color online). (a) Structural model and (b) STM of graphene in registry with the Ni(111) substrate. The grayscale for different Ni layers reveals two different carbon sites A and B causing a threefold symmetry. (c) Insertion of the Au monolayer weakens the $A - B$ contrast but leaves the symmetry predominantly threefold. In addition, a superstructure ($\sim 10 \times 10$) appears. Both effects do not open a substantial band gap ($>$25 meV) below E_F.

Figure 2(b) shows that the passivation of the interface by Au reestablishes $A - B$ symmetry to an extent sufficient for the π band to disperse *linearly* right up to E_F which is met exactly in the Dirac point. This is confirmed in Fig. 2(b) by the faint mirror band (suppressed by interference [21]) dispersing downwards from E_F into the second Brillouin zone in Fig. 2(b) and by the high-resolution ($\sim$25 meV, $\sim$0.2°, $\sim$40 K) measurement in Fig. 2(c). The position of E_F with $E_F = E_D \pm 25$ meV indicates that graphene/Au/Ni(111) may be a better rendering of freestanding graphene than graphene on SiC where the Dirac point appears at 0.45 eV binding energy (and, correspondingly, π at $\bar{\Gamma}$ at $\sim$8.5 eV) [12] or bilayer graphene/SiC with $E_F - E_D = 0.4$ eV [6].

The data presented in Fig. 2(c) confirm that no gap opens up to at least 25 meV below E_F. In fact, we are able to record STM images down to +3 mV bias voltage which, for our room-temperature measurements, again limits the extent of a possible band gap to 25 meV below E_F. The linear dispersion is a distinct signature of relativistic massless charge carriers [2] and its appearance distinguishes monolayer graphene [12] from bilayer graphene with parabolic dispersion [6]. From the constant dE/dk gradient of about 7.5 eV Å we obtain a group velocity of $v_g \sim 1.15 \times 10^6$ m/s or $\sim 1/260$ of the velocity of light in vacuum, c. This is in the range of transport results which yield $\sim c/300$ [2,3].

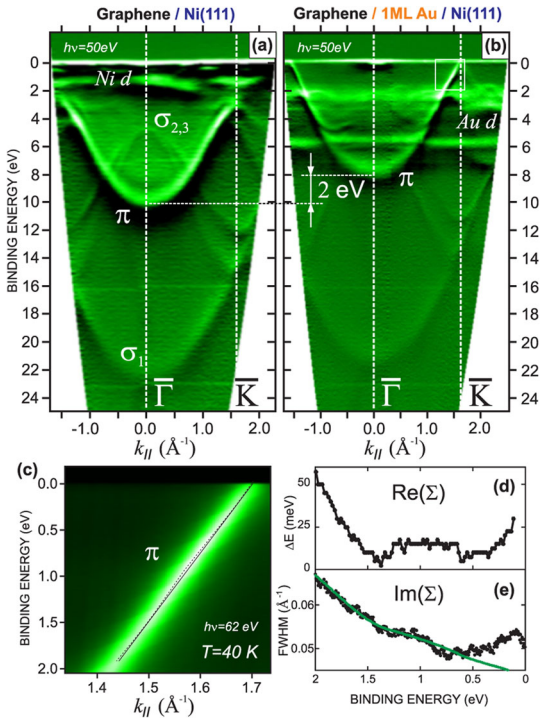

FIG. 2 (color online). Electronic structure of graphene on Ni (111) along $\overline{\Gamma K}$ (a) before and (b)–(e) after intercalation with 1 ML Au leading to a 2 eV shift and the closing of the gap at $\bar{K}$. (c) Dispersion near E_F of π states (dotted line) vs band structure calculation (solid line) and (d) the difference ΔE between the two resulting from a fitting of photoemission peaks, and (e) full peak width at half maximum (FWHM) in momentum space together with a Kramers-Kronig transform of the (d) experimental ΔE (solid line). Renormalization of the band dispersion occurs 0.95 eV below E_F. The photoemission intensity I (c) and its derivative dI/dE (a),(b) are presented.

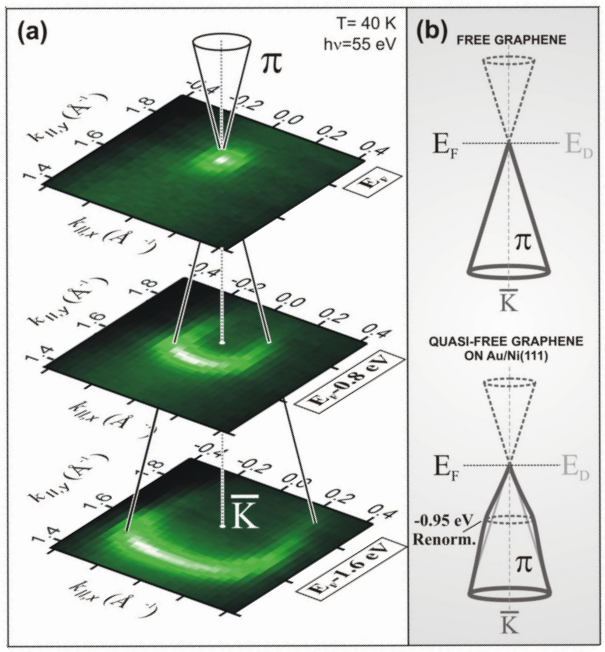

FIG. 3 (color online). (a) The Fermi surface of graphene on Au/Ni(111) is a point at $\bar{K}$, and the π states exhibit a conical relativistic dispersion. (b) Mass renormalization due to interaction with the Au substrate modifies the quasiparticle bands of ideal graphene.

The π band in Fig. 2(a) is not linear and at $\bar{K}$ by almost 1 eV lower than would have been expected from a rigid downward shift of the quasifreestanding graphene bands of Fig. 2(b). This is due to C2p-Ni3d hybridization and the concomitant breaking of the $A-B$ symmetry. There is a current discussion whether the extent to which the $A-B$ symmetry is broken in graphene/SiC suffices to open a band gap of $\sim$260 meV at E_D at $\bar{K}$ [22] or not [23]. We find that in the present system no gap $\geq$25 meV opens below E_F despite the apparent symmetry breaking in the STM. The more relevant criterion for an intact $A-B$ symmetry is perhaps the intensity asymmetry in photoemission [21] which disappears for broken $A-B$ symmetry [24]. The two-dimensional measurements in Fig. 3 do not only prove that there is no gap at $E_F = E_D$, the strong photoemission intensity asymmetry at $E_F - 0.8$ eV and at $E_F - 1.6$ eV shows also that the $A-B$ symmetry is not broken in terms of valence-band interference.

Before proceeding with magnetic properties we want to address two further observations. We find indications for graphene-substrate interaction in an electron-mass renormalization in the $E(\mathbf{k}_\parallel)$ dispersion near E_F. We calculated the band dispersion based on a tight binding model [12] [solid line in Fig. 2(c)] to evaluate from the comparison the experimental real and imaginary parts of the self-energy Σ as shown in Figs. 2(d) and 2(e). A kink appears at 0.95 eV. This feature which does not appear in graphite [11] could be a substrate effect as is frequently being investigated for overlayers [25]. We also observe a structure in the momentum width in Fig. 2(e). The momentum width is a measure of the inverse lifetime or scattering rate of the quasiparticles. With the exception of the region close to E_F which possibly is influenced by superimposed Au and/or Ni emission, the data in Fig. 2(e) are Kramers-Kronig consistent as the Kramers-Kronig transform (solid line) of the data of Fig. 2(d) shows. In particular, the feature at 0.95 eV is reproduced.

A similar behavior has been observed for alkali-doped graphene/SiC caused by plasmon excitation [12]. As the plasmon observed in Ref. [12] is not expected in graphene with $E_D = E_F$, we tend to assign the kink at 0.95 eV to graphene-Au interaction. More work is required to elucidate its origin.

The graphene/Au/Ni(111) system is also characterized by unique magnetic properties. We used spin- and angle-resolved photoemission to analyze the π band near $\bar{K}$. Figure 4(a) shows complete spin-resolved spectra for $\mathbf{k}_\parallel$ along the $\overline{\Gamma K}$ direction. Figure 4(b) zooms in on the π states to reveal a spin splitting of 13 ± 3 meV shown in Fig. 4(c). We verified that the sign of the splitting reverses with the sign of $\mathbf{k}_\parallel$ and is independent of the magnetization

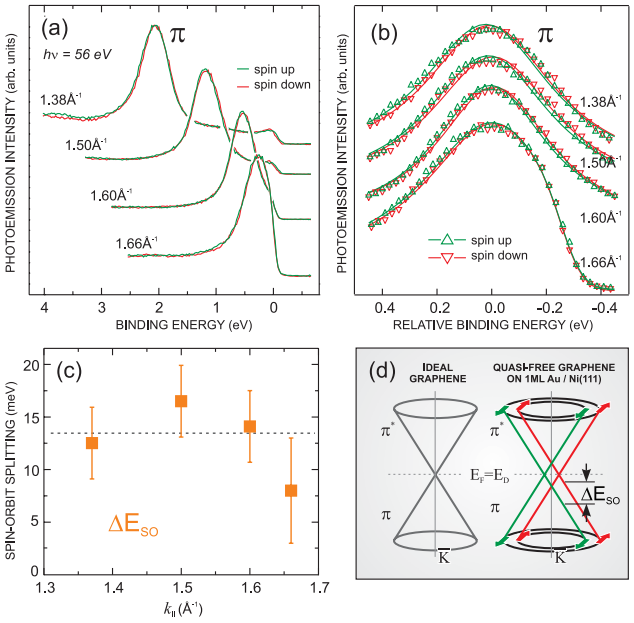

FIG. 4 (color online). Spin-resolved photoemission spectra along $\bar{\Gamma}\bar{K}$ in the vicinity of the Fermi energy. (a) Overview spectra and (b) π states at arbitrary offset. (c) The spin-orbit splitting is constant across the range of $\mathbf{k}_{\parallel}$ points measured. (d) Model for the spin-polarized Fermi surface of graphene.

of the sample. Such type of splitting has been identified before for surface states of heavy metals [26,27] and is identified as Rashba-type spin-orbit splitting. According to Fig. 4(c), the spin-orbit splitting remains largely *constant* across the whole linear part of the π band displayed in Fig. 2(c) including E_F. This is a direct consequence of the unique relativistic, i.e., linear, dispersion in quasifreestanding graphene. As a result, the quasifreestanding graphene prepared here has a spin-orbit-split and spin-polarized Fermi surface [Fig. 4(d)]. The scenario of Fig. 4(d) cannot, at the present resolution, be distinguished from a spin Hall insulator caused by a spin-orbit induced band gap at E_F [28]. In both scenarios, graphene becomes a spin-filter material of high efficiency.

The spin-orbit splitting in graphene has been estimated to be $\sim$0.1 meV [28]. This value is expected to increase in curved graphene, and recently a spin-orbit splitting of 0.37 meV has been measured in carbon nanotubes [29]. Because our Rashba-type spin-orbit splittings are 2 orders of magnitude larger, we conclude that the spin-orbit splitting in graphene is enhanced by a Rashba effect due to the intercalated Au and its high nuclear charge.

A Rashba effect has been reported recently in photoemission spectra of graphene/Ni(111) [30]. An effect on the electron spin was, however, not proven.

In summary, we have shown that quasifreestanding graphene can be produced on Ni(111) by intercalation of Au. The system shows linear dispersion of relativistic Dirac fermions with the Dirac point exactly at the Fermi energy. No gap is observed in photoemission and STM. It was shown that the Au plays the key role in restoring the graphene properties on the Ni substrate. The residual interaction with the Au is revealed, in particular, by a kink in the band dispersion near E_F, a predominantly threefold symmetry in STM, and a $\sim$100-fold enhancement of the spin-orbit splitting of graphene π states.

We would like to thank J. Fink and Th. Seyller for fruitful discussions and A. Vollmer and R. Follath for kind support and acknowledge grants by DFG (No. RA1041/1-1 and No. 436RUS113/735/0-2), RFFI (No. 08-03-00410), and for C. B. and E. V. by the European Union (No. MTKD-CT-2004-003178).

[1] K. S. Novoselov *et al.*, Science **306**, 666 (2004).
[2] K. S. Novoselov *et al.*, Nature (London) **438**, 197 (2005).
[3] Yuanbo Zhang, Yan-Wen Tan, H. L. Stormer, and Philip Kim, Nature (London) **438**, 201 (2005).
[4] S. V. Morozov *et al.*, Phys. Rev. Lett. **100**, 016602 (2008).
[5] M. I. Katsnelson, K. S. Novoselov, and K. Geim, Nature Phys. **2**, 620 (2006).
[6] T. Ohta *et al.*, Science **313**, 951 (2006).
[7] E. V. Castro *et al.*, Phys. Rev. Lett. **99**, 216802 (2007).
[8] S. Sahoo *et al.*, Nature Phys. **1**, 99 (2005).
[9] E. W. Hill *et al.*, IEEE Trans. Magn. **42**, 2694 (2006).
[10] N. Tombros *et al.*, Nature (London) **448**, 571 (2007).
[11] See S. Y. Zhou, G. H. Gweon, and A. Lanzara, Ann. Phys. (N.Y.) **321**, 1730 (2006), and refs. therein.
[12] A. Bostwick *et al.*, Nature Phys. **3**, 36 (2007).
[13] I. Forbeaux, J.-M. Themlin, and J.-M. Debever, Phys. Rev. B **58**, 16 396 (1998).
[14] W.-H. Soe *et al.*, Phys. Rev. B **70**, 115421 (2004).
[15] C. Berger *et al.*, J. Phys. Chem. B **108**, 19912 (2004); Science **312**, 1191 (2006).
[16] E. Rollings *et al.*, J. Phys. Chem. Solids **67**, 2172 (2006).
[17] A. M. Shikin *et al.*, Phys. Rev. B **62**, 13 202 (2000).
[18] G. Bertoni, L. Calmels, A. Altibelli, and V. Serin, Phys. Rev. B **71**, 075402 (2005).
[19] A. M. Shikin *et al.*, Europhys. Lett. **44**, 44 (1998).
[20] G. C. Burnett, T. J. Monroe, and F. B. Dunning, Rev. Sci. Instrum. **65**, 1893 (1994).
[21] E. L. Shirley *et al.*, Phys. Rev. B **51**, 13 614 (1995); F. Matsui *et al.*, Appl. Phys. Lett. **81**, 2556 (2002); S. L. Molodtsov *et al.*, Phys. Rev. B **67**, 115105 (2003).
[22] S. Y. Zhou *et al.*, Nature Mater. **6**, 770 (2007).
[23] E. Rotenberg *et al.*, Nature Mater. **7**, 258 (2008).
[24] A. Bostwick *et al.*, New J. Phys. **9**, 385 (2007).
[25] See, e. g., S. J. Tang, T. Miller, and T. C. Chiang, Phys. Rev. Lett. **96**, 036802 (2006); P. Moras *et al.*, *ibid.* **97**, 206802 (2006).
[26] S. LaShell, B. A. McDougall, and E. Jensen, Phys. Rev. Lett. **77**, 3419 (1996).
[27] See A. M. Shikin *et al.*, Phys. Rev. Lett. **100**, 057601 (2008) and references therein.
[28] C. L. Kane and E. J. Mele, Phys. Rev. Lett. **95**, 226801 (2005).
[29] F. Kuemmeth *et al.*, Nature (London) **452**, 448 (2008).
[30] Yu. S. Dedkov, M. Fonin, U. Rüdiger, and C. Laubschat, Phys. Rev. Lett. **100**, 107602 (2008).